#### **Review**

Lijo P. Mona, Sandile P. Songca, and Peter A. Ajibade\*

# Synthesis and encapsulation of iron oxide nanorods for application in magnetic hyperthermia and photothermal therapy

https://doi.org/10.1515/ntrev-2022-0011 received June 12, 2021; accepted September 27, 2021

Abstract: The synthesis, characterization, and applications of iron oxide nanorods have received attention in recent years. Even though there are several studies on the biological applications of iron oxide nanoparticles, recent studies have shown that rod-shaped iron oxides are effective in magnetic hyperthermia (MHT) as therapeutic technique to treat cancer. This review focused on the synthesis and encapsulation of magnetic iron oxide nanorods (MIONRs) and their use in (MHT) and photothermal therapy (PTT) for cancer cells. Among the synthetic methods that have been used to prepare MIONRs, some could be used to precisely control the particle size of the as-prepared magnetic iron oxide nanoparticles (MIONs), while others could be used to prepare monodisperse particles with uniform size distributions. Some of the results presented in this review showed that magnetic oxide nanorods are more potent in MHT than polyhedralshaped MIONs. The review shows that mixtures of polyhedral- and rod-shaped MIONs resulted in 59 and 77% cell death, while monodisperse MIONRs resulted in 95% cell death. It could thus be concluded that, for magnetic iron oxide to be effective in MHT and PTT, it is important to prepare monodisperse magnetic oxide nanorods.

Sandile P. Songca: University Teaching and Learning Office, University of KwaZulu-Natal, Howard College, Durban 4041, South Africa **Keywords:** encapsulation, iron oxide nanorods, magnetic hyperthermia, photothermal therapy

# 1 Introduction

The synthesis of any magnetic nanoparticles may be carried out either using physical or chemical synthetic techniques [1]. However, several factors such as toxicity and safety associated with administration and accumulation of the materials in body tissues could influence their potential for clinical use [2]. In order to adhere to the safety requirements, a limited concentration of the materials may be used. Magnetic nanoparticles must possess several properties that make them suitable for biomedical applications, these include monodispersity, stability in an aqueous environment, narrow size distributions, and controllable particle size [3]. It is of the utmost importance to ensure the activation of the magnetic nanoparticles, which must be delivered to great depth inside tissues or organs, by means of an external magnet. This can be achieved by the use of frequency and magnetic field strength conditions that are harmless to human body [4]. Metals such as Fe, Co, and Ti can form magnetic oxides and nanocomposites [5]. Studies on magnetic iron oxide nanoparticles (MIONs) focused on their adjustable magnetic properties, low toxicity, and their potential as efficient diagnostic and therapeutic agents [6,7].

Hyperthermia is an experimental treatment for cancer in which heat is induced to elevate the temperature of any part of the body to produce a therapeutic effect [8]. The use of this type of therapeutic technique is receiving attention because cancerous cells are more sensitive to it than normal cells due to the disorder in the vascular structure, which hinders heat transfer [9]. Magnetic hyperthermia (MHT) is a type of hyperthermia that uses magnetic nanoparticles, such as iron oxide nanoparticles, that are administered into the patient's body after which it is subjected to alternating magnetic field [10]. In the case

<sup>\*</sup> Corresponding author: Peter A. Ajibade, School of Chemistry and Physics, University of KwaZulu-Natal, Private Bag X01, Scottsville, Pietermaritzburg, 3209 South Africa, e-mail: ajibadep@ukzn.ac.za Lijo P. Mona: School of Chemistry and Physics, University of KwaZulu-Natal, Private Bag X01, Scottsville, Pietermaritzburg, 3209 South Africa

of photothermal therapy (PTT) near-infrared radiation is used as the initiating energy [11].

#### 1.1 MHT

In MHT, the applied magnetic field enhances the localization/accumulation of the magnetic nanoparticles in the malignant tissues and enhances the selectivity. The alternating magnetic field causes oscillation of the nanoparticles and generates heat that could rise to about 40-43°C in order to kill the malignant tissues [12]. This approach was first reported in 1957 by Gilchrist et al. [13], who injected MIONs into lymphatic channels and subjected them to an alternating magnetic field to generate heat for the destruction of cancer cells. This was proposed after an experiment in which Fe<sub>2</sub>O<sub>3</sub> nanoparticles were delivered to lymph nodes to kill lymphatic metastases, followed by the introduction of an alternating magnetic field, resulting in a 14°C increase in temperature. Jordan et al. [14] revisited the use of nanoparticles to acts as therapeutic agents on tumor cells by injecting the nanoparticles directly to the tumor tissue, and applying an alternating magnetic field to generate heat.

The heat to be absorbed by tissues is generated mainly by the dissipative oscillations of the magnetic moments of the nanoparticles induced by the external oscillating magnetic field [15]. For this reason, factors that affect the amount of heat generated and thus supplied to the tissues include the magnetic nanoparticle size, shape and chemical composition, the dipolar and surface interactions of the nanoparticles as well as the amplitude and frequency of the external magnetic field [16]. A successful MHT treatment is characterized by higher concentration of nanoparticles in the tumor tissue than in the surrounding healthy tissue (selective accumulation) and a high specific absorption rate (SAR) or specific loss power of the particles [17].

Materials that are being used in MHT must be magnetic in nature to be able to respond to external magnetic field, which is introduced in the process. Iron oxide nanoparticles, particularly maghemite (x-Fe<sub>2</sub>O<sub>3</sub>) and magnetite (Fe<sub>3</sub>O<sub>4</sub>) crystalline phases may be used and they constitute MIONs [18,19]. The difference in valency of the ions present in the MION crystal structure gives rise to the inherent magnetic properties. Magnetite, for example, comprises two trivalent ions of iron and a divalent iron ion. The unpaired electron in the iron gives rise to antiparallel magnetic moments that do not cancel each other out, which then produce spontaneous magnetism [20]. In comparison

with other shapes of nanoparticles, Mohapatra et al. observed that nanospheres and nanorods had higher magnetic properties and hyperthermic efficiency [21]. They further reported that rod-shaped superparamagnetic nanoparticles exhibited higher magnetization than their spherical counterparts for the same material type and volume.

In addition to their magnetic properties, magnetic nanoparticles, such as iron oxide, can be used in humans without posing any serious dangers due to their biodegradability. Iron ions in solution can undergo assimilation in the body through a physiological process [22]. The advantages of this technique include non-invasiveness. remote controllability, unlimited penetration depth into the body, molecular level specificity, and nanoscale spatial resolution [23]. The limitations of this technique include the relatively low specific heating power, which raises the need to prepare and use a large amount of nanoparticles [24].

## 1.2 PTT

PTT is a therapeutic technique in which malignant tissues are loaded with nanoparticles, followed by irradiation with a near-infrared laser to generate heat for the destruction of the malignant tissues [25]. This technology is quite promising [26,27] and has a number of advantages, including minimal invasiveness, high specificity, and precise spatialtemporal selectivity [28]. Furthermore, it does not require oxygen and can be carried out with light of longer wavelength (700-1,000 nm), which has less energy and is, therefore, less harmful to the non-malignant surrounding cells. Like MHT, PTT may be carried out using materials in the nanoscale range, at which particles can permeate more and are retained more by the tumor tissues [29,30]. The requirements of a good photothermal agent include good biocompatibility, ability to absorb near-infrared radiation, and a high absorption cross section, which could maximize the conversion of light into heat [31].

Among materials being explored in PTT, gold nanoparticles (AuNPs) have been explored more than nanorods [32-34]. The properties of AuNPs are dependent on the particle shapes and sizes. Gold nanorods (AuNRs) have exhibited extreme sensitivity to changes in their length, width, and aspect ratio. Magnetic nanoparticles with the ability to react to a magnetic field and absorb near-infrared radiation are also good photothermal agents. The inherent magnetic properties also promote the selectivity by the provision of an additional mechanism (magnetic) to accumulate the particles in the tumor cells [35]. Iron oxide

nanoparticles can be used in this technique and other biomedical techniques due to their relatively high biocompatibility, biodegradability, and ease of synthesis and functionalization [36]. MIONs of different shapes such as hexagonal, spherical, and wire-like have been used successfully in the study carried out by Chu *et al.* [37] which are found to be effective in PTT upon using a red and near-infrared laser. In addition, highly crystallized iron oxide nanoparticles are effective in anticancer PTT [38]. Like gold, iron oxide nanorods have a good photothermal conversion efficiency. Furthermore, they have higher photothermal stability and magnetization value [39].

# 2 Methods of synthesis of iron oxide nanoparticles

The challenge in the synthesis of iron oxide nanoparticles is the precise control of the particle size and shape, porosity, crystallinity, and morphology [40]. These characteristics of the as-prepared magnetic oxide nanoparticles depend on the synthetic reaction parameters that may be adjusted to suit the anticipated outcome for a specific application, such as nanorods for application in MHT. It is important to ensure that the method of synthesis is simple, inexpensive, reproducible, and environmentally friendly [41]. All chemical methods are based on the general concept in which the precursor (iron source) is decomposed in a solvent, often in the presence of a ligand. The ligand is responsible for the enhancement of the nanorod suspension, thus preventing aggregation that may be a result of dipolar and van der Waal's interactions [42]. Several methods may be employed for the synthesis of iron oxide nanoparticles, including nanorods, and the most common of these are coprecipitation, sol-gel, microemulsion, and thermal decomposition.

# 2.1 Coprecipitation method

This method entails the mixing of aqueous solutions of iron(II) and iron(III) salts in 1:2 mole ratio followed by the addition of a base such as ammonium hydroxide to precipitate the iron ions as hydroxides (equation (1)) [43] at an elevated temperature in an inert atmosphere to get a black magnetic precipitate in the magnetite form. At room temperature, magnetite easily reacts with atmospheric oxygen to form maghemite, as illustrated in equation (2) [44].

$$Fe^{2+} + 2Fe^{3+} + 8OH^{-} \rightarrow Fe_{3}O_{4} + H_{2}O_{3}$$
 (1)

$$2Fe_3O_4 + 0.5O_2 \rightarrow 3Fe_2O_3$$
. (2)

The coprecipitation method is the most cost-effective and convenient method to prepare magnetic iron oxide nanorods (MIONRs) and provides relatively high yields [45]. The desired shape and dimensions of a nanoparticle may be obtained by controlling several reaction parameters, such as pH, temperature, stirring rate, and concentrations of solute and surfactant [46]. The advantages of the coprecipitation method include ease of operation, low equipment requirements, time-effectiveness, and relatively high yield [47].

# 2.2 Sol-gel

This method entails the formation of a colloidal solution (sol) of the precursor and its conversion into a gel inside reverse micelles, followed by heating by calcination or reflux treatments as illustrated in Figure 1. First, a sol of the metal (iron) precursor may be converted to a wet gel by using a proton scavenger within the reverse micelle. The gel is then washed with a polar solvent for the removal of impurities that include excess surfactants and dried in air. Crystallization (2) may be induced by high-temperature treatment of the gel powder in a high boiling point reducing solvent [48].

## 2.3 Microemulsion

This method involves the use of two immiscible liquids with a layer of surfactants at the interface, thus forming an emulsion of high thermal stability. When two identical emulsions that contain the precursors of the desired

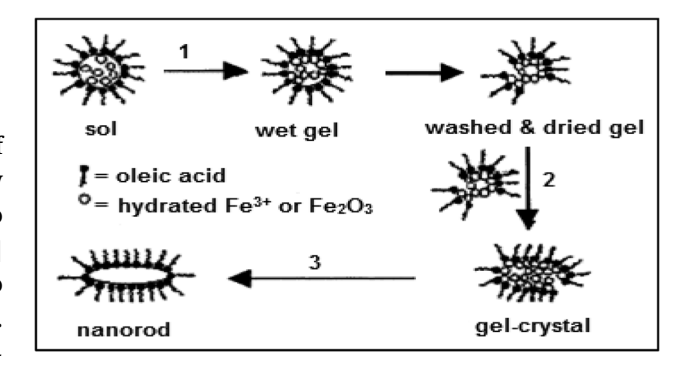


**Figure 1:** Schematic presentation of the formation of nanorods in the sol-gel method [48].

nanoparticles are mixed, the collision takes place continuously, and so does coalescence and breaking of micro-droplets [49]. This results in precipitation of micelles. The nanoparticles that exist in the micelles may be recovered by addition of solvents. As illustrated in Figure 2, in this technique, a microemulsion containing the salt of the metal is usually mixed with another microemulsion containing a reducing agent (A) or the reducing agent may be added directly in a solid (B) or a gaseous state (C) [50]. Schulman *et al.* [51] used this method of nanoparticle synthesis in 1959 to prepare nanomaterials in a homogenous, stable solution of water, benzene, hexanol, and k-oleate.

# 2.4 Thermal decomposition

The thermal decomposition method of synthesis involves the decomposition of organometallic or metal salt precursors at high temperature (up to about 400°C). The particle size may be controlled by variation in the decomposition temperature, reaction time, and the concentration of the precursor [52]. In the case of iron oxide

nanoparticles, the commonly known precursors include iron(III) oleate (Fe(C<sub>18</sub>H<sub>33</sub>O<sub>2</sub>)<sub>3</sub>), iron oxyhydroxide (FeOOH), iron pentacarbonyl (Fe(CO)<sub>5</sub>), and iron(III) acetyl acetonate (Fe(acac)/Fe(C<sub>5</sub>H<sub>7</sub>O<sub>2</sub>)<sub>3</sub>) [53,54]. These precursors are used with organic solvents, such as benzyl ether and ethylene diamine, and surfactants [55]. Some examples of work carried out through the techniques discussed above are summarized in Table 1.

# 3 Synthesis of iron oxide nanorods

# 3.1 Low aspect ratio nanorods

Nath *et al.* [66] reported the synthesis of MIONRs by using acidic solutions of iron(II) chloride tetrahydrate and iron (III) chloride hexahydrate and ammonium hydroxide to adjust the pH. While the aspect ratio was as low as 2.3, the as-prepared nanorods were very long (310  $\pm$  10 nm) and wide (135  $\pm$  5 nm). de Montferrand *et al.* [67] reported the microwave-assisted preparation of magnetite nanorods

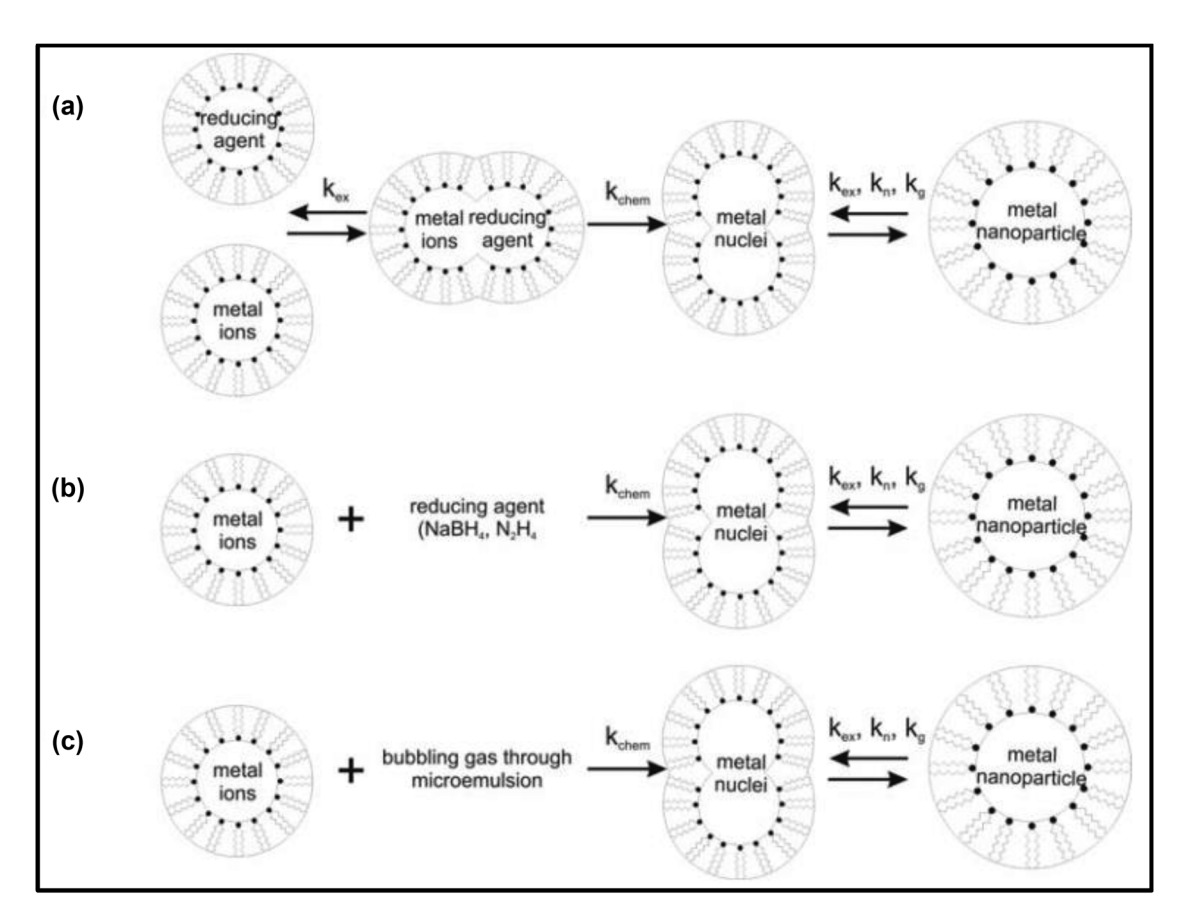


Figure 2: A schematic presentation of preparation of nanoparticles by microemulsion methods [50].

180 — Lijo P. Mona et al. DE GRUYTER

Table 1: Methods of iron oxide prepared using some of these methods and the morphology and phase properties of the nanoparticles

Method of synthesis	Morphology of the product	Phase of iron oxide	References
Coprecipitation	Spherical	Maghemite	Hui and Salimi [56]
	Rod-shaped and cubic	Magnetite	Khalil [57]
	Spherical and octahedral	Magnetite	Roth <i>et al</i> . [58]
Sol-gel	Rod-shaped	Maghemite	Woo et al. [59]
	Spherical	Magnetite, maghemite, and hematite	Cui <i>et al</i> . [60]
Microemulsion	Hexagonal	Hematite	Wongwailikhit and Horwongsakul [61]
	Spherical	Magnetite	Koutzarova et al. [62]
Thermal decomposition	Spherical	Maghemite	Jović Orsini et al. [63]
	Prismatic	Maghemite	Sharma and Jeevanandam [64]
	Spherical	Magnetite	Belaid et al. [65]

by reduction of iron(III) oxyhydroxide nanorods prepared by hydrolysis of iron(III) chloride in the presence of polyethylenimine (PEI), at different concentrations, using hydrazine as the reducing agent. The average length of the nanorods was 38 nm, and the width was 12 nm. Kumar *et al.* [68] fabricated magnetite nanorods by ultrasound irradiation of iron(II) acetate in the presence of  $\beta$ -cyclodextrin, which served as a size-stabilizing agent. This method, however, yielded nanorods of low aspect ratio (3.4), each with a length of 48 nm and a width of 14 nm, with very little agglomeration.

Woo *et al.* [59] fabricated hematite nanorods through this method by use of iron(III) chloride precursor, with oleic acid as the surfactant. The mole ratio of water to oleic acid was varied, and the aspect ratios varied between 3.2 and 3.6. Khan *et al.* [69] used iron(III) oxyhydroxide to synthesize magnetic oxide nanospheres by coprecipitation, followed by their calcination to produce Fe<sub>2</sub>O<sub>3</sub> nanorods. The nanorods with length and width ranges of 110–120 and 25–40 nm, respectively, were obtained. In a different approach, Geng *et al.* [70] synthesized magnetite nanorods by the synthesis of  $\beta$ -FeOOH nanorods followed by their reduction. The magnetite nanorods of length 45 nm and width 10 nm (aspect ratio = 4.5) exhibited a high SAR of 1,072 W/g at 33 kA/m at a concentration of 5 mg/mL in water.

## 3.2 Medium aspect ratio nanorods

Xu *et al.* [71] reported precise size-controlled synthesis of MIONRs. The method involved the preparation of β-FeOOH nanorods and their treatment with oleic acid and oleylamine. The as-prepared nanorods' lengths ranged from 25 to 85 nm with aspect ratios between 5 and 6. The MIONRs exhibited a relatively high cell uptake than spherically shaped particles. A time- and cost-effective method for

the synthesis of hematite nanorods was reported by Ramzannezhad and Bahari [72] in which the iron(III) chloride precursor was used with sodium hydroxide and cetyltrimethylammonium bromide (CTAB) as a surfactant. In this method, the CTAB concentration was observed to be inversely proportional to the nanorod length, with average length ranging between 25 and 32 nm. Orza et al. [73] used a simple one-step procedure in an inert atmosphere (N<sub>2</sub> or argon) with a standard Schlenk line setup. They used mixtures of iron(III) acetylacetonate with PEI in the presence of oleylamine and phenyl ether. The synthesis yielded nanorods of lengths about 25 and 50 nm with diameters of 5 and 8 nm and aspect ratios of about 5 and 6.3, respectively. Another one-step method was reported by Xu and Zhang [74], in which α-Fe<sub>2</sub>O<sub>3</sub> nanorods were synthesized through hydrothermal treatment of iron(III) chloride in aqueous formamide solution. While a 24 h treatment yielded octahedral-shaped particles, a 12 h treatment yielded nanorods with lengths in the range of 50-100 nm that are 10-30 nm wide, with aspect ratios of 4-8.

Mohapatra et al. [21] used the same method as de Montferrand et al. [67] although they did not use a microwave oven. Iron(III) oxyhydroxide nanorods were prepared by hydrolysis of iron(III) chloride in the presence of PEI at different concentrations. These nanorods were reduced by the use of oleylamine to yield magnetite nanorods of lengths 25-70 nm with diameters of 3-12 nm. Si et al. [75] reported a facile solvothermal method to synthesize single-crystal magnetite nanorods with lengths in the range of 58-250 nm and widths in the range of 8-64 nm. Sayed and Polshettiwar [76] devised a method in which iron(II) sulfate was used as a precursor, taking the goethite route. The as-synthesized nanorods had average length of 270–315 and 30–35 nm in width. Chaudhari et al. [77] reported a simple synthetic route in which  $\beta$ -FeOOH nanorods were first fabricated by hydrolysis of iron(III) chloride hexahydrate in the presence of caffeine. The use of ethanol as a co-solvent yielded  $\beta$ -FeOOH nanorod with aspect ratios up to 10. The  $\beta$ -FeOOH nanorods were then calcined slowly to form Fe<sub>2</sub>O<sub>3</sub> nanorods, while the morphology was not affected significantly.

# 3.3 High aspect ratio nanorods

A thermal decomposition method was used by Wang and Yang [78] to prepare magnetic iron oxide nanorods using iron pentacarbonyl as a precursor in an imidazolium ionic liquid. The nanorods showed uniformity in terms of size, with aspect ratio of  $10 \pm 1$ . Marins  $et\ al.$  [79] synthesized iron oxide nanorods of uniform size, with aspect ratios of 10 and 5.2. In a two-step synthetic procedure, akaganeite was synthesized and reduced with hydrazine in a microwave reactor to yield the MIONRs. In a different approach, Kloust  $et\ al.$  [80] devised a simple method for the synthesis of maghemite nanorods in which iron oleate dots were used. The average length of the resultant nanorods was 24 nm while the width was 2.5 nm, with an aspect ratio of about 10. The width of the nanorods was observed to be directly proportional to the reaction temperature and time.

Dixit and Jeevanandam [81] carried out thermal decomposition of iron(III) acetylacetonate (Fe(acac)<sub>3</sub>) in diphenyl ether in the presence of oleic acid and different concentrations

of oleyl amine. Sphere-like particles were obtained with lower concentrations of oleyl amine, while higher concentrations of oleyl amine yielded rod-like structures of about 500 nm in length, up to the micro-scale with 50–150 nm diameters and aspect ratios up to 10. They suggested that oleyl amine concentration controls the morphology of the particles in this method. Sun *et al.* [82] synthesized magnetite nanorods by addition of hexadecylamine and oleic acid to n-octanol at 50°C and addition of Fe(CO)<sub>5</sub> to the resultant solution after cooling. The size and aspect ratio were improved as transmission electron microscopy (TEM) images showed nanorods of length  $63 \pm 5$  nm with a diameter of  $6.5 \pm 2$  nm. An increase in the mass of hexadecylamine yielded nanorods of a greater size and aspect ratio (11.7), with 140 nm length and 12 nm diameter.

The procedure devised by Sun *et al.* [82] was followed by Das *et al.* [83], as shown in Figure 3, with a few modifications. The amounts were doubled, except for hexadecylamine, which was added in different amounts. The nanorods had lengths of 41, 65, and 56 nm with diameters of 7, 5.7, and 10 nm, respectively, and aspect ratios up to 11. Nanorods with 11 aspect ratios exhibited a high SAR of 862 W/g in water, while the SAR increased to about 1.3 kW/g when the nanorods were aligned.

Park *et al.* [84] synthesized iron oxide nanorods of length 11 nm and a 2 nm width using spherical iron nanoparticles by thermal decomposition of Fe(CO)<sub>5</sub> in the

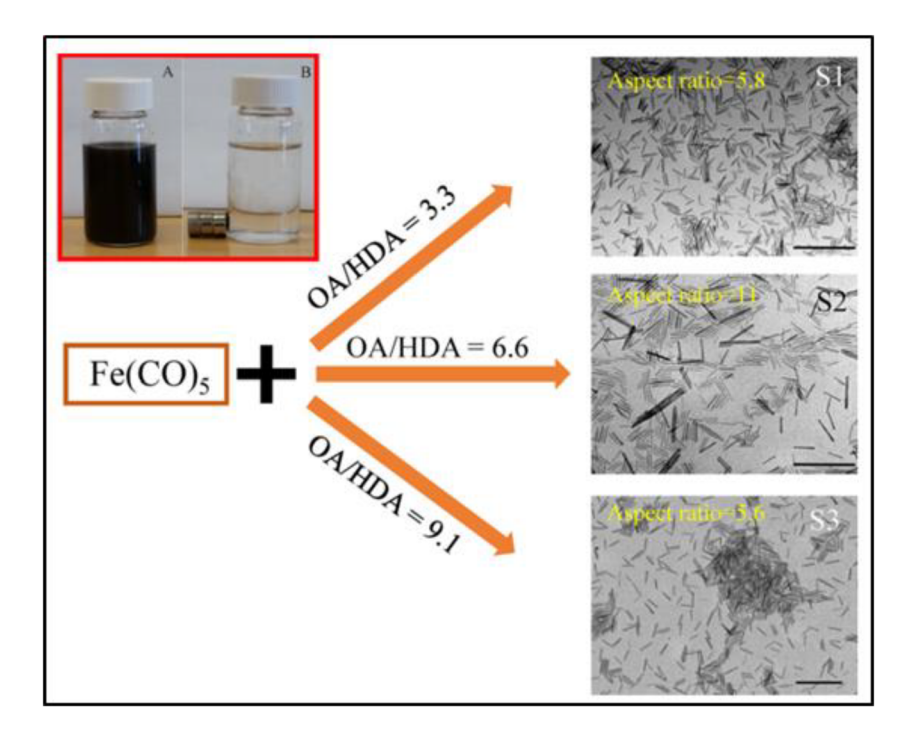


Figure 3: Scheme for the synthesis of magnetite nanorods with tunable aspect ratios. Nanorods are monodispersed in A in the absence of a magnet, while B shows the same nanorods with an external magnet [83].

presence of trioctylphosphine oxide at 340°C. The use of didodecyldimethylammonium in pyridine increased the length of the nanorods to 22 and 27 nm while the width did not change, thus giving aspect ratios as high as 13.5. Duong et al. [85] reported the synthesis of high aspect ratio (15) nanorods by centrifugal deposition. They used iron(III) nitrate nonahydrate as the precursor and centrifugation was used to settle the precipitated nanorods. The length of the nanorods was about 150 nm, while the diameter ranged from 10 to 20 nm. Upon testing the nanorods for magnetic hyperthermic efficiency, a great temperature increase was observed in about 2s after applying the external magnetic field to generate heat of 1.93 W/mm<sup>2</sup>. Bao et al. [86] also reported a facile method of preparation of single-crystalline y-Fe<sub>2</sub>O<sub>3</sub> nanorods by using inexpensive precursors that are non-toxic such as iron oleate. The nanorod width varied directly with the reaction temperature. When reaction was carried out at temperature of 200-240°C, the length remained in the same range of 30-40 nm with width ranging between 2 and 5 nm, with aspect ratios of up to 20. However, a higher reaction temperature yielded nanorods of length 50 nm and width 10 nm. For the same aspect ratio, Lian et al. [87] synthesized magnetite nanorods through hydrolysis of iron(III) chloride and iron(II) sulfate solutions containing urea at 90-95°C. The nanorods were up to 1 µm long and had diameters ranging between 40 and 50 nm.

# 4 Encapsulation of MIONRs

Like other nanoparticles, MIONRs possess large surface area to volume ratio. The large ratio causes dipole-dipole magnetic interactions which give rise to agglomeration in order to minimize the surface energies [88]. Agglomeration of the particles causes significant reduction in the intrinsic superparamagnetic properties. A suspension of iron oxide nanorods without surface modification is susceptible to surface oxidation, resulting in the loss of magnetism. Magnetite is mostly affected because it could be easily oxidized than other iron oxides.

With appropriate surface properties, superparamagnetic iron oxide nanorods possess many properties that make them useful in biomedical applications, including magnetic resonance imaging, hyperthermia, and drug delivery [89]. The encapsulation of nanorods, or generally, the modification of nanoparticles aids in improving the stability and dispersion of the magnetic nanorods, their physicochemical and mechanical properties, their surface activity, and their biocompatibility [90,91]. In addition, the encapsulation of nanorods increases the

possibility of further functionalization with other materials that are suitable for the intended applications [92]. The materials that may be used for encapsulation of magnetic iron includes small organic molecules, polymers, biomolecules, and inorganic materials such as silica, elementary metals or non-metals, metal oxides, and sulfides [93].

Many polymers have been used for the encapsulation of nanorods [94–96], but among them, poly(ethyleneglycol) is the most commonly used polymer in drug delivery systems [97,98] due to its properties: (a) easy renal excretion; (b) low interfacial free energy water; (c) excluded volume effect; (d) non-immunogenic properties, and (e) non-antigenic properties [99]. Moreover, poly(ethylene glycol) (PEG)-coated nanorods have the ability to interact with cell membranes without causing harm to the active proteins and cells, thus enhancing the cellular response. Other polymers that have been used widely for the encapsulation of MIONRs are dextran [100], chitosan, poly acid polyetherimide, PEI, polydopamine, polyvinyl alcohol, and alginate. Dextran has exhibited great biocompatibility and solubility in water and reduction of saturation magnetization of MIONs [101].

The methods of encapsulation are generally classified into two groups, namely dry and wet methods. Dry methods include physical vapor deposition, plasma treatment, pyrolysis of organic materials (polymeric or monomeric organic materials) for in situ precipitation, and chemical vapor deposition [102]. The commonly used wet coating methods are sol-gel processes, emulsification, and solvent evaporation. The latter involves the emulsification of the polymer in aqueous phase and the use of a volatile organic solvent for the purpose of dispersion [103]. The solvent may then be evaporated by means of heating, continuous stirring, or vacuum. When the solvent evaporates, the polymer precipitates onto the surfaces of the nanoparticles, thereby forming a shell [104].

Nath *et al.* [66] carried out the facile encapsulation of freshly prepared iron oxide nanorods by the addition of an aqueous solution of dextran. The dextran-coated nanorods exhibited superparamagnetic properties and improved water spin-spin relaxation. Orza et al. [73] carried out the encapsulation of MIONs with poly(ethylene glycol) with terminal amine groups (PEG-NH<sub>2</sub>) as proposed by Fang et al. [105]. As-prepared MIONRs were salinized, washed with hexane, and treated with a solution of PEG-NH<sub>2</sub> in tetrahydrofuran followed by sonication. A different approach referred to as layer-by-layer technique, involving adsorption of cationic and anionic polymers in an alternating manner, was followed by Reyes-Ortega et al.; first, a layer of PEI by pH adjustment is formed followed by sonication in the presence of a PEI solution [106]. The

PEI-coated nanorods were mixed with an aqueous solution of poly(sodium 4-styrenesulphonate) (PSS), and sonicated. Characterization with fourier-transform infrared spectroscopy (FTIR) confirmed the presence of two layers of PEI and PSS. The coated nanorods were stable and generally effective in hyperthermia. Ahmad et al. [107] functionalized magnetite nanorods with a semi-essential amino acid, L-arginine, at room temperature, by sonication. FTIR and XPS analyses proved the success of functionalization.

Encapsulation of iron oxide nanorods with pluronic F127 poly(ethylene oxide)-poly(propylene oxide)-poly (ethylene oxide) block copolymer was reported by Dehvari et al. [108]. The copolymer was ultrasonicated with MIONRs in methanol and emulsification was carried out in PBS. Nguyen et al. [109] reported the encapsulation of MIONRs with a copolymer of methyl methacrylate and n-butyl acrylate, by ultrasonication, using the water-soluble initiator, 4,4'-azobis(4-cyanopentanoic acid). The nanorods maintained their magnetic properties after encapsulation.

The coating of MIONRs with oleic acid was carried out by Sharma et al. [110]. To a suspension of magnetite nanorods, a solution of oleic acid was added dropwise up to a ratio of 1:1 with the suspension of nanorods. TEM images indicated successful coating with good dispersion. Yu et al. [111] coated MIONRs of high porosity with NH<sub>2</sub>-PEG-FA to produce folic acid-conjugated iron oxide nanorods (FA-PEG-MIONR). Doxorubicin was loaded on to these coated nanorods and tests performed in vitro indicated cytotoxicity to HeLa cells.

Although limited research has been carried out on MIONRs, many methods of encapsulation have been reported on MIONs of other forms, especially nanospheres. Hypothetically, the methods have a high probability of being successful on MIONRs. Feuser et al. [112] used poly (methyl methacrylate) to encapsulate MIONs coated in oleic acid, by miniemulsion polymerization in the presence of lecithin, miglyol, and azobisisobutyronitrile. The encapsulation was efficient and superparamagnetic properties were observed and the as-prepared MIONRs show improvement in their biocompatibility. In vitro experiments in which AC magnetic field was introduced in the presence of the encapsulated MIONs resulted in a significant decrease in the viability of U87MG cells.

Predescu et al. [113] carried out encapsulation by the use of dextran, a polysaccharide polymer. Aqueous solutions of dextran of different concentrations were mixed with magnetite nanoparticles and stirred at an elevated temperature. Successful encapsulation was confirmed by Scanning electron microscopy (SEM) and FTIR techniques. Sadhasivam et al. [114] reported surface modification of carbon-encapsulated iron oxide nanoparticles with a layer of poly(ethylene glycol) conjugated to folic acid (PEG-FA). Khoee and Kavand [115] modified MIONs, although spherical with mPEG end-capped with acrylate groups. The previously prepared acrylated mPEG was dissolved in anhydrous dimethylformamide together with 3-aminopropyl triethoxysilane and the solution was stored for 3 days at room temperature.

Encapsulation of MIONs, by hydrophobic interaction, with polyaspartamide was reported by Nguyen et al. [116]. The encapsulated nanoparticles exhibited good biocompatibility and good hyperthermic efficiency against 4T1 cancer cells in vitro and in vivo. Xu et al. [117] carried out the encapsulation with polyacrylamide. A suspension of MIONs was mixed with acrylamide and N,N'-methylene bis (acrylamide) followed by ultrasonication of the mixture. The polyacrylamide-encapsulated nanoparticles were recommended for biological applications, owing to their dispersity in water and superparamagnetic behavior. Patsula et al. [118] reported the PEGylation of MIONs by use of a PEG-containing bisphosphonate anchoring group. Upon characterization, the PEG layer was observed as a brush-like shell that successfully prevented aggregation of the MIONs. MIONs capped with oleic acid were encapsulated by Xue et al., [119] using phosphorylated mPEG in chloroform. These PEG-MIONs exhibited excellent biocompatibility.

Nemec et al. [120] encapsulated citric acid-stabilized MIONs in silica shells with a thickness range of 3-5 nm. This was carried out by hydrolysis of tetraethoxysilane followed by condensation of silica precursors on the nanoparticles' surfaces. In comparison, the heating capacity, in PTT, of the encapsulated MIONs was higher than the bare MIONs, giving respective temperatures of 45.7 and 43.5°C. In MHT, MION and MION-SIL did not exhibit any significant difference in heating efficiency. Lee et al. carried out the encapsulation with poly(D,L-lactide-co-glycolide) (PLGA), by an emulsification-diffusion method, in which an aqueous solution of PLGA was emulsified in ethyl acetate and the organic solvent was extracted into the aqueous phase [121]. The smaller nanoparticles exhibited higher magnetic susceptibility.

# 5 Characterization of as-prepared and encapsulated iron oxide nanorods

Characterization is an important step that follows every step of synthesis in order to assess the success in the formation of the desired product as well as its properties. It is equally important to characterize the products after encapsulation to evaluate the success and the extent of coating of the nanorods with the polymer of preference. SEM and TEM are techniques used to determine the morphology, size and size distributions of nanoparticles as well as the dispersion [122–124]. The lengths and width/diameter of a nanorod may be determined by means of these techniques and from these the aspect ratio may be calculated. TEM is capable of characterizing at a higher resolution than SEM [125,126]. Figure 4 shows a set of TEM images of AuNRs with different dimensions, with clearly visible morphology. Images A and C have the smallest nanorods and were magnified twice as much as the other specimens to be visible.

A vibrating sample magnetometer (VSM) may be used for the determination of the magnetic properties of MIONRs [128,129]. In the VSM, a sample is exposed to a uniform magnetic field and subjected to a vibration perpendicular to the magnetic field [130]. The magnetization or magnetic moment per mass of nanoparticles may be measured for a well quantified magnetic field and from this a magnetization curve may be plotted to study the behavior of the MIONRs [131]. FTIR may be used for the characterization of the as-prepared nanorods and the encapsulated ones [132]. The differences in the spectra, particularly in the wavenumber of the characteristic peaks, may be used to determine whether the encapsulation is successful.

Figure 5 shows FTIR spectra of magnetite nanoparticles (a), PEG (e), and magnetite encapsulated with different amounts of PEG: 1 g (b), 2 g (c), and 3 g (d) [133]. Increasing the amount of PEG used resulted in the shifting of the C=O absorption bands from 1,617 to 1,624/cm, thus suggesting coordination through the carbonyl group in the PEG.

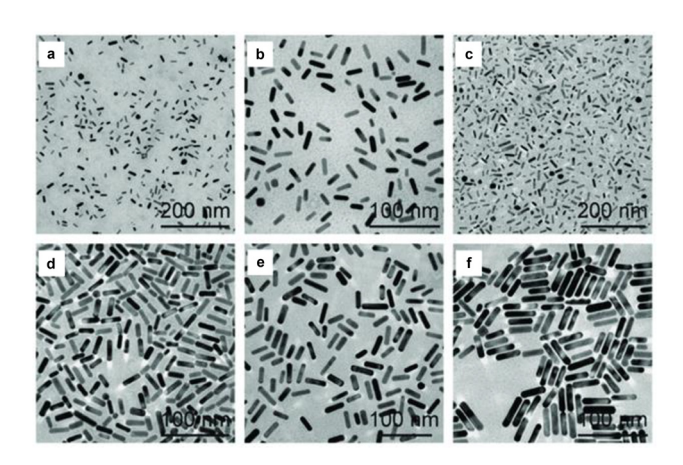
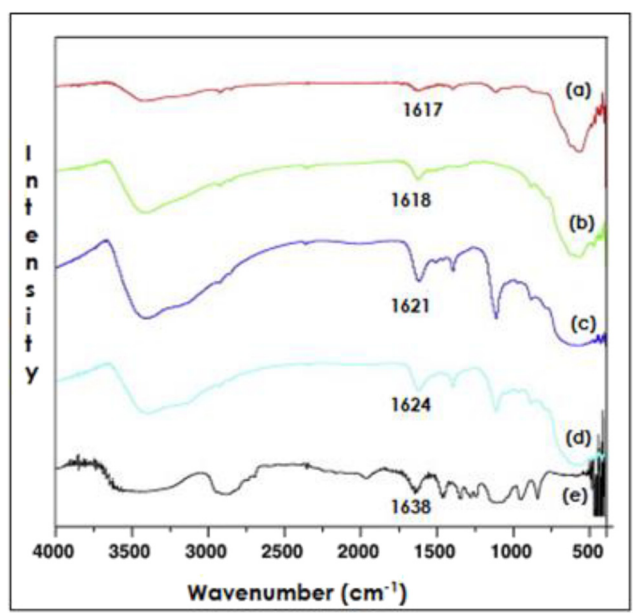


Figure 4: TEM images of AuNRs of different sizes [127].

# 6 Application of encapsulated iron oxide nanorods in PTT and MHT

MIONs of different morphologies have been used for *in vitro* and *in vivo* experiments with great success, exhibiting potential to kill cancer cells *in vitro* and to reduce the size of the tumor significantly *in vivo* [134–136]. However, there is a growing interest in rod-shaped iron oxide nanoparticles, although not much work has been reported on their application in MHT and PTT. Recent studies have explored the potential of iron oxide nanoparticles in PTT, where it shows obvious advantages over AuNPs [137,138]. Due to their magnetic properties, iron oxide nanoparticles have also been used for MHT, but rod-shaped nanoparticles was found to be effective in PTT with dual plasmonic resonance [139,140] which enhances the heat generation.

Nikitin *et al.* [141] carried out *in vitro* MHT experiments using MIONRs in sorbitol on 4T1 mouse breast cancer cells. The mixture was exposed to alternating magnetic field of high frequency (261–393 kHz) and strength (20 kA/m) with 95% cell death. The use of two mixtures of nanorods and nanopolyhedra resulted in 77 and 59% cell death. Bilici *et al.* [142] used poly-acrylic acid-encapsulated superparamagnetic iron oxide nanoparticles for PTT on HeLa cells using a 795 nm laser. The cell viability was observed to have decreased to 20.75% after the treatment. Nemec *et al.* [120] carried out a series of PTT and MHT experiments using monodispersed and clustered iron oxide



**Figure 5:** FTIR spectra of (a)  $Fe_3O_4$ , (b)  $PEG(1g)/Fe_3O_4$ , (c)  $PEG(2g)/Fe_3O_4$ , (d)  $PEG(3g)/Fe_3O_4$ , and (e) PEG[133].

nanoparticles with and without silica coatings. Fe concentrations in the range of 1-150 mM were explored in this study, while using an 808 nm laser with the power density of 0.3 W/cm<sup>2</sup> for PTT and a magnetic field strength of 18 mT at a frequency of 471 kHz for MHT. The silica-coated nanoparticles exhibited the highest photothermal efficiency followed by monodispersed nanorods and lastly by clustered nanorods. For MHT, the highest increase in temperature was observed for monodispersed nanoparticles, followed by those that were coated in silica, and finally by the clus-

Magnetite nanoparticles doped with vttrium (for enhancement of magnetic properties) were used by Kowalik et al. [143] for MHT. Exposure of 4T1 cells to magnetic field in the presence of MIONs led to reduction in cell viability by 15% only, while the use of yttrium-doped magnetite nanoparticles led to a reduction in cell viability by 77%. Calatayud et al. carried out MHT using MIONs on BV2 microglial micro-tumor phantoms [144]. The sudden effect of the MHT resulted in a drop of cell viability to 70% at 46°C. After treatment for 4.5 h, the cell viability decreased to 25%. Salimi et al. [145] carried out in vivo MHT treatment of breast cancer-bearing mice using MIONs functionalized with poly amidoamine dendrimers of the fourth generation. After 27 days of treatment, the tumor volume had decreased to 23.7% of the initial volume.

# 7 Conclusion

The syntheses of MIONRs have been carried out, using different techniques, for practical applications in MHT and PTT. These methods used to prepare the magnetic iron oxide nanorods lead to the formation of MIONRs with different sizes and aspect ratios in the range of 2.3–20. Some of these methods could be used to precisely control the particle size, while others could produce monodisperse particles with uniform size distributions. It has been shown that the magnetic iron oxide nanorods with high aspect ratio increases the SAR. At higher temperature, particles with an aspect ratio of 15 could be prepared and there is a direct proportionality between aspect ratio and SAR. Studies have shown that SAR increases by about 50% with increase in aspect ratio from 6 to 11. Polymer-encapsulation of iron oxide nanorods with nanoparticles of other morphologies has been explored much more than that of nanorods. However, there is evidence that the methods used for the preparation of spherical nanoparticles could be modified to prepare rod-shaped nanoparticles. The review showed that magnetic oxide

nanorods are more potent in MHT than polyhedral nanoparticles. A mixture of nanorods and nano-polyhedral resulted in 59 and 77% cell death, whereas monodisperse nanorods resulted in 95% cell death. Research on the synthesis and encapsulation of rod-shaped iron oxide nanoparticles could be explored more in order to improve the aspect ratio of the materials and their use in MHT and PTT. The use of iron oxide nanorods for MHT and PTT has the potential to transform the clinical applications by further enhancement of cell death and improved selectivity with minimal invasiveness. Development of these techniques and its adoption could reduce the number of people that require chemotherapeutic treatments.

**Funding information:** The authors acknowledge financial support from the National Research Foundation.

Author contributions: All authors have accepted responsibility for the entire content of this manuscript and approved its submission.

**Conflict of interest:** The authors state no conflict of interest.

# References

- [1] Majidi S, Sehrig FZ, Farkhani SM, Goloujeh MS, Akbarzadeh A. Current methods for synthesis of magnetic nanoparticles. Artif Cells Nanomed Biotechnol. 2016;44(2):722-34.
- [2] Ajdary M, Moosavi MA, Rahmati M, Falahati M, Mahboubi M, Mandegary A, et al. Health concerns of various nanoparticles: a review of their in vitro and in vivo toxicity. Nanomaterials. 2018:8(9):634.
- Xu Y, Zhu Y. Synthesis of magnetic nanoparticles for biomedical applications. Nano Adv. 2016;1:25-38.
- [4] Hergt R, Dutz S. Magnetic particle hyperthermia-biophysical limitations of a visionary tumour therapy. J Magnetism Magnetic Mater. 2007;311(1):187-92.
- [5] Li X, Wei J, Aifantis KE, Fan Y, Feng Q, Cui FZ, et al. Current investigations into magnetic nanoparticles for biomedical applications. J Biomed Mater Res A. 2016;104(5):1285-96.
- Dadfar SM, Roemhild K, Drude NI, von Stillfried S, Knüchel R, [6] Kiessling F, et al. Iron oxide nanoparticles: diagnostic, therapeutic and theranostic applications. Adv Drug Delivery Rev. 2019;138:302-25.
- [7] Weinstein JS, Varallyay CG, Dosa E, Gahramanov S, Hamilton B, Rooney WD, et al. Superparamagnetic iron oxide nanoparticles: diagnostic magnetic resonance imaging and potential therapeutic applications in neurooncology and central nervous system inflammatory pathologies, a review. J Cereb Blood Flow Metab. 2010;30(1):15-35.
- [8] Issels RD. Hyperthermia adds to chemotherapy. Eur J Cancer. 2008;44(17):2546-54.

- [9] Chung EJ, Leon L, Rinaldi C. Nanoparticles for biomedical applications: fundamental concepts, biological interactions and clinical applications. Amsterdam, Netherlands: Elsevier; 2019.
- [10] Mahmoudi K, Bouras A, Bozec D, Ivkov R, Hadjipanayis C. Magnetic hyperthermia therapy for the treatment of glioblastoma: a review of the therapy's history, efficacy and application in humans. Int J Hyperth. 2018;34(8):1316-28.
- [11] Shan G, Weissleder R, Hilderbrand SA. Upconverting organic dye doped core-shell nano-composites for dual-modality NIR imaging and photo-thermal therapy. Theranostics. 2013;3(4):267-74.
- Wust P, Hildebrandt B, Sreenivasa G, Rau B, Gellermann J, Riess H. et al. Hyperthermia in combined treatment of cancer. Lancet Oncol. 2002;3(8):487-97.
- Gilchrist RK, Medal R, Shorey WD, Hanselman RC, Parrott JC, Taylor CB. Selective inductive heating of lymph nodes. Ann Surg. 1957;146(4):596-606.
- Jordan A, Wust P, Fähling H, John W, Hinz A, Felix R. Inductive heating of ferrimagnetic particles and magnetic fluids: physical evaluation of their potential for hyperthermia. Int J Hyperth. 1993;9(1):51-68.
- [15] Suto M, Hirota Y, Mamiya H, Fujita A, Kasuya R, Tohji K, et al. Heat dissipation mechanism of magnetite nanoparticles in magnetic fluid hyperthermia. J Magnetism Magnetic Mater. 2009;321(10):1493-6.
- [16] Cruz MM, Ferreira LP, Alves AF, Mendo SG, Ferreira P, Godinho M, et al. Nanoparticles for magnetic hyperthermia, in nanostructures for cancer therapy. Amsterdam, Netherlands: Elsevier; 2017. p. 485-511.
- [17] Giustini AJ, Petryk AA, Cassim SM, Tate JA, Baker I, Hoopes PJ. Magnetic nanoparticle hyperthermia in cancer treatment. Nano Life. 2010;1(01n02):17-32.
- [18] Maenosono S, Saita S. Theoretical assessment of FePt nanoparticles as heating elements for magnetic hyperthermia. IEEE Trans Magnetic. 2006;42(6):1638-42.
- Hilger I. In vivo applications of magnetic nanoparticle hyperthermia. Int J Hyperth. 2013;29(8):828-34.
- Chang D, Lim M, Goos JACM, Qiao R, Ng YY, Mansfeld FM, et al. Biologically targeted magnetic hyperthermia: potential and limitations. Front Pharmacol. 2018;9:831.
- [21] Mohapatra J, Mitra A, Tyagi H, Bahadur D, Aslam M. Iron oxide nanorods as high-performance magnetic resonance imaging contrast agents. Nanoscale. 2015;7(20):9174-84.
- Mohapatra S, Nguyen TA, Nguyen-Tri P. Noble metal-metal oxide hybrid nanoparticles: fundamentals and applications. Amsterdam, Netherlands: Elsevier; 2018.
- [23] Cazares-Cortes E, Cabana S, Boitard C, Nehlig E, Griffete N, Fresnais J, et al. Recent insights in magnetic hyperthermia: from the "hot-spot" effect for local delivery to combined magneto-photo-thermia using magneto-plasmonic hybrids. Adv Drug Delivery Rev. 2019;138:233-46.
- [24] Fratila RM, De La Fuente JM. Nanomaterials for magnetic and optical hyperthermia applications. Amsterdam, Netherlands: Elsevier: 2018.
- [25] Doughty A, Hoover AR, Layton E, Murray CK, Howard EW, Chen WR. Nanomaterial applications in photothermal therapy for cancer. Materials. 2019;12(5):779.
- Tsai M-F, Chang SH, Cheng FY, Shanmugam V, Cheng YS, Su CH, et al. Au nanorod design as light-absorber in the first

- and second biological near-infrared windows for in vivo photothermal therapy. ACS Nano. 2013;7(6):5330-42.
- [27] Akhavan O, Ghaderi E. Graphene nanomesh promises extremely efficient in vivo photothermal therapy. Small. 2013;9(21):3593-601.
- [28] Zou L, Wang H, He B, Zeng L, Tan T, Cao H, et al. Current approaches of photothermal therapy in treating cancer metastasis with nanotherapeutics. Theranostics. 2016;6(6):762-72.
- [29] Maeda H, Wu J, Sawa T, Matsumura Y, Hori K. Tumor vascular permeability and the EPR effect in macromolecular therapeutics: a review. J Controlled Rel. 2000;65(1-2):271-84.
- [30] Vert M, Doi Y, Hellwich KH, Hess M, Hodge P, Kubisa P, et al. Terminology for biorelated polymers and applications (IUPAC recommendations 2012). Pure Appl Chem. 2012;84(2):377-410.
- Melamed JR, Edelstein RS, Day ES. Elucidating the funda-[31] mental mechanisms of cell death triggered by photothermal therapy. ACS Nano. 2015;9(1):6-11.
- [32] Hwang S, Nam J, Jung S, Song J, Doh H, Kim S. Gold nanoparticle-mediated photothermal therapy: current status and future perspective. Nanomed. 2014;9(13):2003-22.
- [33] Kim J, Park S, Lee JE, Jin SM, Lee JH, Lee IS, et al. Designed fabrication of multifunctional magnetic gold nanoshells and their application to magnetic resonance imaging and photothermal therapy. Angew Chem. 2006;118(46):7918-22.
- [34] Ahmad R, Fu J, He N, Li S. Advanced gold nanomaterials for photothermal therapy of cancer. J Nanosci Nanotechnol. 2016;16(1):67-80.
- [35] Estelrich J, Busquets MA. Iron oxide nanoparticles in photothermal therapy. Molecules. 2018;23(7):1567.
- [36] Revia RA, Zhang M. Magnetite nanoparticles for cancer diagnosis, treatment, and treatment monitoring: recent advances. Mater Today. 2016;19(3):157-68.
- Chu M, Shao Y, Peng J, Dai X, Li H, Wu Q, et al. Near-infrared laser light mediated cancer therapy by photothermal effect of Fe<sub>3</sub>O<sub>4</sub> magnetic nanoparticles. Biomaterials. 2013;34(16):4078-88.
- Chen H, Burnett J, Zhang F, Zhang J, Paholak H, Sun D. Highly crystallized iron oxide nanoparticles as effective and biodegradable mediators for photothermal cancer therapy. J Mater Chem B. 2014;2(7):757-65.
- [39] Zhou Z, Sun Y, Shen J, Wei J, Yu C, Kong B, et al. Iron/iron oxide core/shell nanoparticles for magnetic targeting MRI and near-infrared photothermal therapy. Biomaterials. 2014;35(26):7470-8.
- [40] Campos EA, Stockler Pinto DVB, Oliveira JIS, Mattos EDC, Dutra RDCL. Synthesis, characterization and applications of iron oxide nanoparticles-a short review. J Aerosp Technol Manag. 2015;7(3):267-76.
- [41] Moacă EA, Coricovac ED, Soica CM, Pinzaru IA, Păcurariu CS, Dehelean CA. Preclinical aspects on magnetic iron oxide nanoparticles and their interventions as anticancer agents: enucleation, apoptosis and other mechanism. Iron Ores Iron Oxide Materials, Volodymyr Shatokha, IntechOpen. 2018;229-54. doi: 10.5772/intechopen.74176.
- [42] Korotcenkov G. Iron oxide nanoparticles for biomedical applications: synthesis, functionalization and application. Amsterdam, Netherlands: Elsevier; 2017.
- [43] Al-Alawy AF, Al-Abodi EE, Kadhim RM. Synthesis and characterization of magnetic iron oxide nanoparticles by co-

- precipitation method at different conditions. J Eng. 2018;24(10):60-72.
- Laurent S, Forge D, Port M, Roch A, Robic C, Vander Elst L, et al. [44] Magnetic iron oxide nanoparticles: synthesis, stabilization, vectorization, physicochemical characterizations, and biological applications. Chem Rev. 2008;108(6):2064-110.
- [45] Li Y, Wang J, Feng B, Duan K, Weng J. Synthesis and characterization of antimony-doped tin oxide (ATO) nanoparticles with high conductivity using a facile ammonia-diffusion coprecipitation method. J Alloy Compd. 2015;634:37-42.
- Tyagi H, Kushwaha A, Kumar A, Aslam M. A facile pH controlled citrate-based reduction method for gold nanoparticle synthesis at room temperature. Nanoscale Res Lett. 2016;11(1):1-11.
- Ling W, Wang M, Xiong C, Xie D, Chen Q, Chu X, et al. Synthesis, surface modification, and applications of magnetic iron oxide nanoparticles. J Mater Res. 2019;34(11):1828-44.
- [48] Prescott WV, Schwartz Al. Nanorods, nanotubes, and nanomaterials research progress. New York, United States: Nova Publishers; 2008.
- [49] Kalarikkal N, Thomas S, Koshy O. Nanomaterials: physical, chemical, and biological applications. Florida, United States: CRC Press; 2018.
- [50] Zieliska-Jurek A, Reszczyska J, Grabowska E, Zalesk A. Nanoparticles preparation using microemulsion systems, Microemulsions - An introduction to properties and applications, Dr. Reza Najjar, editor. InTech; 2012;229-50. ISBN: 978-953-51-0247-2.
- Schulman JH, Stoeckenius W, Prince LM. Mechanism of for-[51] mation and structure of micro emulsions by electron microscopy. J Phys Chem. 1959;63(10):1677-80.
- Vashist A, Kaushik AK, Ahmad S, Nair M. Nanogels for biomedical applications. London, United Kingdom: Royal Society of Chemistry; 2017.
- Hufschmid R, Arami H, Ferguson RM, Gonzales M, Teeman E, Brush LN, et al. Synthesis of phase-pure and monodisperse iron oxide nanoparticles by thermal decomposition. Nanoscale. 2015;7(25):11142-54.
- [54] Wetterskog E, Agthe M, Mayence A, Grins J, Wang D, Rana S, et al. Precise control over shape and size of iron oxide nanocrystals suitable for assembly into ordered particle arrays. Sci Technol Adv Mater. 2014;15(5):055010.
- [55] Arndt D, Zielasek V, Dreher W, Bäumer M. Ethylene diamineassisted synthesis of iron oxide nanoparticles in high-boiling polyolys. J Colloid Interface Sci. 2014;417:188-98.
- [56] Hui BH, Salimi MN. Production of iron oxide nanoparticles by co-precipitation method with optimization studies of processing temperature, pH and stirring rate. IOP Conference Series: Materials Science and Engineering. London, United Kingdom: IOP Publishing; 2020.
- [57] Khalil MI. Co-precipitation in aqueous solution synthesis of magnetite nanoparticles using iron(III) salts as precursors. Arab J Chem. 2015;8(2):279-84.
- Roth H-C, Schwaminger SP, Schindler M, Wagner FE, [58] Berensmeier S. Influencing factors in the CO-precipitation process of superparamagnetic iron oxide nano particles: a model based study. J Magnetism Magnetic Mater. 2015;377:81-9.
- Woo K, Lee HJ, Ahn JP, Park YS. Sol-gel mediated synthesis of Fe<sub>2</sub>O<sub>3</sub> nanorods. Adv Mater. 2003;15(20):1761-4.

- [60] Cui H, Liu Y, Ren W. Structure switch between α-Fe<sub>2</sub>O<sub>3</sub>, y-Fe<sub>2</sub>O<sub>3</sub> and Fe<sub>3</sub>O<sub>4</sub> during the large scale and low temperature sol-gel synthesis of nearly monodispersed iron oxide nanoparticles. Adv Powder Technol. 2013;24(1):93-7.
- [61] Wongwailikhit K, Horwongsakul S. The preparation of iron(III) oxide nanoparticles using W/O microemulsion. Mater Lett. 2011;65(17):2820-2.
- Koutzarova T, Kolev S, Ghelev C, Paneva D, Nedkov I. [62] Microstructural study and size control of iron oxide nanoparticles produced by microemulsion technique. Phys Status Solidi c. 2006;3(5):1302-7.
- [63] Jović Orsini N, Babić-Stojić B, Spasojević V, Calatayud MP, Cvjetićanin N, Goya GF. Magnetic and power absorption measurements on iron oxide nanoparticles synthesized by thermal decomposition of Fe(acac)3. J Magnetism Magnetic Mater. 2018;449:286-96.
- Sharma G, Jeevanandam P. Synthesis of self-assembled prismatic iron oxide nanoparticles by a novel thermal decomposition route. RSC Adv. 2013;3(1):189-200.
- [65] Belaïd S, Laurent S, Vermeech M, Vander Elst L, Perez-Morga D, Muller RN. A new approach to follow the formation of iron oxide nanoparticles synthesized by thermal decomposition. Nanotechnology. 2013;24(5):055705.
- [66] Nath S, Kaittanis C, Ramachandran V, Dalal N, Perez JM. Synthesis, magnetic characterization, and sensing applications of novel dextran-coated iron oxide nanorods. Chem Mater. 2009;21(8):1761-7.
- de Montferrand C, Hu L, Milosevic I, Russier V, Bonnin D, [67] Motte L, et al. Iron oxide nanoparticles with sizes, shapes and compositions resulting in different magnetization signatures as potential labels for multiparametric detection. Acta Biomaterialia. 2013;9(4):6150-7.
- [68] Kumar RV, Koltypin Y, Xu XN, Yeshurun Y, Gedanken A, Felner I. Fabrication of magnetite nanorods by ultrasound irradiation. J Appl Phys. 2001;89(11):6324-8.
- [69] Khan SR, Jamil S, Ashraf Janjua MRS, Khera RA. Synthesis of ferric oxyhydroxide nanoparticles and ferric oxide nanorods by reflux assisted coprecipitation method and comparative study of their thermal properties. Mater Res Express. 2017:4(11):115019.
- [70] Geng S, Yang H, Ren X, Liu Y, He S, Zhou J, et al. Anisotropic magnetite nanorods for enhanced magnetic hyperthermia. Chemistry-An Asian J. 2016;11(21):2996-3000.
- Xu Y, Wu H, Xiong Q, Ji B, Yi H, Duan H, et al. Size-controllable [71] magnetic iron oxide nanorods for biomarker targeting and improving microfluidic mixing. ACS Appl Bio Mater. 2019;2(8):3362-71.
- [72] Ramzannezhad A, Bahari A. Synthesis and tuning of hematite  $(\alpha-Fe_2O_3)$  iron oxide nanorods with magnetism. J Superconductivity Nov Magnetism. 2018;31(7):2247-53.
- Orza A, Wu H, Xu Y, Lu Q, Mao H. One-step facile synthesis of [73] highly magnetic and surface functionalized iron oxide nanorods for biomarker-targeted applications. ACS Appl Mater Interfaces. 2017;9(24):20719-27.
- [74] Xu H, Wang X, Zhang L. Selective preparation of nanorods and micro-octahedrons of Fe<sub>2</sub>O<sub>3</sub> and their catalytic performances for thermal decomposition of ammonium perchlorate. Powder Technol. 2008;185(2):176-80.
- Si J-C, Xing Y, Peng ML, Zhang C, Buske N, Chen C, et al. [75] Solvothermal synthesis of tunable iron oxide nanorods and

- their transfer from organic phase to water phase. Cryst Eng Comm. 2014;16(4):512-6.
- [76] Sayed FN, Polshettiwar V. Facile and sustainable synthesis of shaped iron oxide nanoparticles: effect of iron precursor salts on the shapes of iron oxides. Sci Rep. 2015;5(1):1-14.
- Chaudhari NK, Fang B, Bae TS, Yu JS. Low temperature synthesis of single crystalline iron hydroxide and oxide nanorods in aqueous media. I Nanosci Nanotechnol. 2011:11(5):4457-62.
- Wang Y, Yang H. Synthesis of iron oxide nanorods and nanocubes in an imidazolium ionic liquid. Chem Eng J. 2009;147(1):71-8.
- Marins JA, Montagnon T, Ezzaier H, Hurel C, Sandre O, Baltrunas D, et al. Colloidal stability of aqueous suspensions of polymer-coated iron oxide nanorods: implications for biomedical applications. ACS Appl Nano Mater. 2018;1(12):6760-72.
- Kloust H, Zierold R, Merkl JP, Schmidtke C, Feld A, Pöselt E, [08] et al. Synthesis of iron oxide nanorods using a template mediated approach. Chem Mater. 2015;27(14):4914-7.
- Dixit S, Jeevanandam P. Synthesis of iron oxide nanoparticles by thermal decomposition approach. In Advanced materials research. Bach, Switzerland: Trans Tech Publications Ltd: 2009.
- [82] Sun H, Chen B, Jiao X, Jiang Z, Qin Z, Chen D. Solvothermal synthesis of tunable electroactive magnetite nanorods by controlling the side reaction. J Phys Chem C. 2012;116(9):5476-81.
- Das R, Alonso J, Nemati Porshokouh Z, Kalappattil V, [83] Torres D, Phan MH, et al. Tunable high aspect ratio iron oxide nanorods for enhanced hyperthermia. J Phys Chem C. 2016;120(18):10086-93.
- Park S-J, Kim S, Lee S, Khim ZG, Char K, Hyeon T. Synthesis and magnetic studies of uniform iron nanorods and nanospheres. J Am Chem Soc. 2000;122(35):8581-2.
- Duong E, Chan S, Gan Y, Zhang L. Centrifugal deposition of iron oxide magnetic nanorods for hyperthermia application. J Therm Eng. 2015;1(2):99-103.
- Bao L, Low WL, Jiang J, Ying JY. Colloidal synthesis of magnetic nanorods with tunable aspect ratios. I Mater Chem. 2012:22(15):7117-20.
- Lian S, Wang E, Kang Z, Bai Y, Gao L, Jiang M, et al. Synthesis of magnetite nanorods and porous hematite nanorods. Solid State Commun. 2004;129(8):485-90.
- Wu W, He Q, Jiang C. Magnetic iron oxide nanoparticles: synthesis and surface functionalization strategies. Nanoscale Res Lett. 2008;3(11):397-415.
- Bloemen M, Brullot W, Luong TT, Geukens N, Gils A, [89] Verbiest T. Improved functionalization of oleic acid-coated iron oxide nanoparticles for biomedical applications. J Nanopart Res. 2012;14(9):1-10.
- Zhu N, Ji H, Yu P, Niu J, Farooq M, Akram M, et al. Surface modification of magnetic iron oxide nanoparticles. Nanomaterials. 2018;8(10):810.
- Wu W, Wu Z, Yu T, Jiang C, Kim WS. Recent progress on [91] magnetic iron oxide nanoparticles: synthesis, surface functional strategies and biomedical applications. Sci Technol Adv Mater. 2015;16:023501.
- [92] Sun SN, Wei C, Zhu ZZ, Hou YL, Venkatraman SS, Xu ZC. Magnetic iron oxide nanoparticles: synthesis and surface

- coating techniques for biomedical applications. Chin Phys B. 2014;23(3):037503.
- [93] Khan I, Saeed K, Khan I. Nanoparticles: properties, applications and toxicities. Arab J Chem. 2019;12(7):908-31.
- [94] Gole A, Murphy CJ. Polyelectrolyte-coated gold nanorods: synthesis, characterization and immobilization. Chem Mater. 2005;17(6):1325-30.
- [95] Ravirajan P, Peiró AM, Nazeeruddin MK, Graetzel M, Bradley DD, Durrant JR, et al. Hybrid polymer/zinc oxide photovoltaic devices with vertically oriented ZnO nanorods and an amphiphilic molecular interface layer. J Phys Chem B. 2006;110(15):7635-9.
- [96] Hotchkiss JW, Lowe AB, Boyes SG. Surface modification of gold nanorods with polymers synthesized by reversible addition-fragmentation chain transfer polymerization. Chem Mater. 2007;19(1):6-13.
- [97] D'souza AA, Shegokar R. Polyethylene glycol (PEG): a versatile polymer for pharmaceutical applications. Expert Opin Drug Delivery. 2016;13(9):1257-75.
- [98] Knop K, Hoogenboom R, Fischer D, Schubert US. Poly(ethylene glycol) in drug delivery: pros and cons as well as potential alternatives. Angew Chem Int Ed. 2010;49(36):6288-308.
- [99] Gölander CG, Herron JN, Lim K, Claesson P, Stenius P, Andrade JD. Properties of immobilized PEG films and the interaction with proteins. Poly(ethyleneglycol) Chemistry. Boston, MA: Springer; 1992. p. 221-45.
- [100] Carmen Bautista M, Bomati-Miguel O, del Puerto Morales M, Serna CJ, Veintemillas-Verdaguer S. Surface characterisation of dextran-coated iron oxide nanoparticles prepared by laser pyrolysis and coprecipitation. J Magnetism Magnetic Mater. 2005;293(1):20-7.
- [101] Shaterabadi Z, Nabiyouni G, Soleymani M. High impact of in situ dextran coating on biocompatibility, stability and magnetic properties of iron oxide nanoparticles. Mater Sci Eng C. 2017;75:947-56.
- [102] Wang Y, Dave RN, Pfeffer R. Polymer coating/encapsulation of nanoparticles using a supercritical anti-solvent process. J Supercrit Fluids. 2004;28(1):85-99.
- [103] Gundloori RV, Singam A, Killi N. Nanobased intravenous and transdermal drug delivery systems. In Applications of targeted nano drugs and delivery systems. Amsterdam, Netherlands: Elsevier; 2019. p. 551-94.
- [104] Urban M, Musyanovych A, Landfester K. Fluorescent superparamagnetic polylactide nanoparticles by combination of miniemulsion and emulsion/solvent evaporation techniques. Macromol Chem Phys. 2009;210(11):961-70.
- [105] Fang C, Bhattarai N, Sun C, Zhang M. Functionalized nanoparticles with long-term stability in biological media. Small. 2009;5(14):1637-41.
- Reyes-Ortega F, Checa Fernández BL, Delgado AV, Iglesias GR. Hyperthermia-triggered doxorubicin release from polymer-coated magnetic nanorods. Pharmaceutics. 2019;11(10):517.
- [107] Ahmad N, Ahmad M, Aslam M, Singh SN, Talwar SS. Synthesis of arginine functionalized iron oxide nanorods. Adv Sci Eng Med. 2012;4(2):132-6.
- [108] Dehvari K, Chen Y, Tsai YH, Tseng SH, Lin KS. Superparamagnetic iron oxide nanorod carriers for paclitaxel

- delivery in the treatment and imaging of colon cancer in mice. J Biomed Nanotechnol. 2016;12(9):1734-45.
- [109] Nguyen D, Pham BTT, Huynh V, Kim BJ, Pham NTH, Bickley SA, et al. Monodispersed polymer encapsulated superparamagnetic iron oxide nanoparticles for cell labeling. Polymer. 2016;106:238-48.
- [110] Sharma A, Baral D, Bohidar HB, Solanki PR. Oxalic acid capped iron oxide nanorods as a sensing platform. Chemicobiol Interact. 2015;238:129-37.
- [111] Yu P, Xia XM, Wu M, Cui C, Zhang Y, Liu L, et al. Folic acidconjugated iron oxide porous nanorods loaded with doxorubicin for targeted drug delivery. Colloids Surf B Biointerf. 2014;120:142-51.
- [112] Feuser PE, Bubniak LS, Silva MCS, Viegas AC, Castilho Fernandes A, Ricci-Junior E, et al. Encapsulation of magnetic nanoparticles in poly(methyl methacrylate) by miniemulsion and evaluation of hyperthermia in U87MG cells. Eur Polym J. 2015;68:355-65.
- [113] Predescu AM, Matei E, Berbecaru AC, Pantilimon C, Drăgan C, Vidu R, et al. Synthesis and characterization of dextrancoated iron oxide nanoparticles. R Soc Open Sci. 2018;5(3):171525.
- [114] Sadhasivam S, Savitha S, Wu CJ, Lin FH, Stobiński L. Carbon encapsulated iron oxide nanoparticles surface engineered with polyethylene glycol-folic acid to induce selective hyperthermia in folate over expressed cancer cells. Int J Pharmaceutics. 2015;480(1-2):8-14.
- [115] Khoee S, Kavand A. A new procedure for preparation of polyethylene glycol-grafted magnetic iron oxide nanoparticles. J Nanostructure Chem. 2014;4(3):1-6.
- [116] Nguyen MP, Nguyen MH, Kim J, Kim D. Encapsulation of superparamagnetic iron oxide nanoparticles with polyaspartamide biopolymer for hyperthermia therapy. Eur Polym J. 2020:122:109396.
- [117] Xu ZZ, Wang CC, Yang WL, Deng YH, Fu SK. Encapsulation of nanosized magnetic iron oxide by polyacrylamide via inverse miniemulsion polymerization. J Magnetism Magnetic Mater. 2004;277(1-2):136-43.
- [118] Patsula V, Horák D, Kučka J, Macková H, Lobaz V, Francová P, et al. Synthesis and modification of uniform PEG-neridronate-modified magnetic nanoparticles determines prolonged blood circulation and biodistribution in a mouse preclinical model. Sci Rep. 2019;9(1):1-12.
- [119] Xue W, Liu Y, Zhang N, Yao Y, Ma P, Wen H, et al. Effects of core size and PEG coating layer of iron oxide nanoparticles on the distribution and metabolism in mice. Int J Nanomed. 2018;13:5719-31.
- [120] Nemec S, Kralj S, Wilhelm C, Abou-Hassan A, Rols MP, Kolosnjaj-Tabi J. Comparison of iron oxide nanoparticles in photothermia and magnetic hyperthermia: effects of clustering and silica encapsulation on nanoparticles' heating yield. Appl Sci. 2020;10(20):7322.
- [121] Lee S-J, Jeong JR, Shin SC, Kim JC, Chang YH, Lee KH, et al. Magnetic enhancement of iron oxide nanoparticles encapsulated with poly(D,L-latide-co-glycolide). Colloids Surf A: Physicochem Eng Asp. 2005;255(1-3):19-25.
- [122] Huang X, Teng X, Chen D, Tang F, He J. The effect of the shape of mesoporous silica nanoparticles on cellular uptake and cell function. Biomaterials. 2010;31(3):438-48.

- [123] Kálomista I, Kéri A, Ungor D, Csapó E, Dékány I, Prohaska T, et al. Dimensional characterization of gold nanorods by combining millisecond and microsecond temporal resolution single particle ICP-MS measurements. J Anal At Spectromet. 2017;32(12):2455-62.
- [124] Asadi Asadabad M, Jafari Eskandari M. Transmission electron microscopy as best technique for characterization in nanotechnology. Synth React Inorg Metal-Org Nano-Metal Chem. 2015;45(3):323-6.
- [125] Johari O. Comparison of transmission electron microscopy and scanning electron microscopy of fracture surfaces. JOM. 1968;20(6):26-32.
- [126] Arenas-Alatorre J, Silva-Velazquez Y, Alva Medina A, Rivera M. Advantages and limitations of OM, SEM, TEM and AFM in the study of ancient decorated pottery. Appl Phys A. 2010;98(3):617-24.
- [127] An L, Wang Y, Tian Q, Yang S. Small gold nanorods: recent advances in synthesis, biological imaging, and cancer therapy. Materials. 2017;10(12):1372.
- [128] Wang Y, Kaur P, Tan AT, Singh R, Lee PC, Springham SV, et al. Iron oxide magnetic nanoparticles synthesized by atmospheric microplasmas. In International Journal of Modern Physics: Conference Series. Singapore: World Scientific; 2014.
- [129] Araujo JFDF, Costa MC, Louro SRW, Bruno AC. A portable Hall magnetometer probe for characterization of magnetic iron oxide nanoparticles. J Magnetism Magnetic Mater. 2017;426:159-62.
- [130] Foner S. Versatile and sensitive vibrating-sample magnetometer. Rev Sci Instrum. 1959;30(7):548-57.
- [131] Maldonado-Camargo L, Unni M, Rinaldi C. Magnetic characterization of iron oxide nanoparticles for biomedical applications. In Biomedical nanotechnology. Berlin, Germany: Springer; 2017. p. 47-71
- [132] Yue-Jian C, Juan T, Fei X, Jia-Bi Z, Ning G, Yi-Hua Z, et al. Synthesis, self-assembly, and characterization of PEGcoated iron oxide nanoparticles as potential MRI contrast agent. Drug Dev Ind Pharm. 2010;36(10):1235-44.
- Anbarasu M, Anandan M, Chinnasamy E, Gopinath V, [133] Balamurugan K. Synthesis and characterization of polyethylene glycol (PEG) coated Fe<sub>3</sub>O<sub>4</sub> nanoparticles by chemical coprecipitation method for biomedical applications. Spectrochimica Acta A Mol Biomol Spectrosc. 2015;135:536-9.
- [134] Balivada S, Rachakatla RS, Wang H, Samarakoon TN, Dani RK, Pyle M, et al. A/C magnetic hyperthermia of melanoma mediated by iron(0)/iron oxide core/shell magnetic nanoparticles: a mouse study. BMC Cancer. 2010;10(1):119.
- [135] Rego G, Nucci MP, Mamani JB, Oliveira FA, Marti LC, Filgueiras IS, et al. Therapeutic efficiency of multiple applications of magnetic hyperthermia technique in glioblastoma using aminosilane coated iron oxide nanoparticles: in vitro and in vivo study. Int J Mol Sci. 2020;21(3):958.
- $[136]\ \ \mbox{Yu}\ \mbox{Q, Xiong XQ, Zhao}\ \mbox{L, Xu}\ \mbox{TT, Bi}\ \mbox{H, Fu}\ \mbox{R, et al.}\ \mbox{Biodistribution}$ and toxicity assessment of superparamagnetic iron oxide nanoparticles in vitro and in vivo. Curr Med Sci. 2018;38(6):1096-102.
- [137] Riley RS, Day ES. Gold nanoparticle-mediated photothermal therapy: applications and opportunities for multimodal

- cancer treatment. Wiley Interdiscip Rev Nanomed Nanobiotechnol. 2017;9(4):e1449.
- [138] Van de Broek B, Devoogdt N, D'Hollander A, Gijs HL, Jans K, Lagae L, et al. Specific cell targeting with nanobody conjugated branched gold nanoparticles for photothermal therapy. ACS Nano. 2011;5(6):4319-28.
- [139] Link S, El-Sayed MA. Shape and size dependence of radiative, non-radiative and photothermal properties of gold nanocrystals. Int Rev Phys Chem. 2000;19(3):409-53.
- [140] Ros I, Placido T, Amendola V, Marinzi C, Manfredi N, Comparelli R, et al. SERS properties of gold nanorods at resonance with molecular, transverse, and longitudinal plasmon excitations. Plasmonics. 2014;9(3):581-93.
- [141] Nikitin A, Khramtsov M, Garanina A, Mogilnikov P, Sviridenkova N, Shchetinin I, et al. Synthesis of iron oxide nanorods for enhanced magnetic hyperthermia. J Magnetism Magnetic Mater. 2019;469:443-9.

- [142] Bilici K, Muti A, Demir Duman F, Sennaroğlu A, Yağcı Acar H. Investigation of the factors affecting the photothermal therapy potential of small iron oxide nanoparticles over the 730-840 nm spectral region. Photochem Photobiol Sci. 2018;17(11):1787-93.
- Kowalik P, Mikulski J, Borodziuk A, Duda M, Kamińska I, Zajdel K, et al. Yttrium-doped iron oxide nanoparticles for magnetic hyperthermia applications. J Phys Chem C. 2020;124(12):6871-83.
- [144] Calatayud MP, Soler E, Torres TE, Campos-Gonzalez E, Junquera C, Ibarra MR, et al. Cell damage produced by magnetic fluid hyperthermia on microglial BV2 cells. Sci Rep. 2017;7(1):1-16.
- [145] Salimi M, Sarkar S, Saber R, Delavari H, Alizadeh AM, Mulder HT. Magnetic hyperthermia of breast cancer cells and MRI relaxometry with dendrimer-coated iron-oxide nanoparticles. Cancer Nanotechnol. 2018;9(1):1-19.